Smectic ordering of homogeneous semiflexible polymers

Raul Cruz Hidalgo* and D. E. Sullivan
Department of Physics, University of Guelph, Guelph, Ontario, Canada N1G2W1

Jeff Z. Y. Chen
Department of Physics, University of Waterloo, Waterloo, Ontario, Canada N2L3G1
(Received 25 November 2004; published 22 April 2005)

A self-consistent-field theory for fluids of homogeneous wormlike polymers exhibiting a one-dimensional spatial variation is presented. We have extended the treatment of excluded-volume effects by adding an effective interaction term which describes the excluded volume between wormlike cylindrical segments and terminal (or end) segments of the polymer molecules. This enables us to find a smectic-A phase in the case of homogeneous semiflexible polymers. Using this framework, we have investigated the occurrence of smectic-A, nematic, and isotropic phases in the second-virial (Onsager) approximation. Phase diagrams are calculated for systems characterized by different rigidities (i.e., persistence lengths). For the case of infinitely rigid molecules, the nematic-smectic transition appears to be mostly second order. Systems of semiflexible molecules exhibit mainly a first-order smectic-nematic transition, and their isotropic-nematic-smectic triple points are accessed for different rigidity values. The nematic-smectic transition line is in good agreement with previous analytical calculations, which were also performed assuming the second-virial approximation. However, the values of the volume fraction at the nematic-smectic transition are large compared with computer simulation results, indicating limitations of the second-virial approximation.

DOI: 10.1103/PhysRevE.71.041804 PACS number(s): 61.25.Hq, 64.70.Md

I. INTRODUCTION

The importance of anisotropic repulsive interactions for stabilizing liquid-crystalline phases in model fluids is well known [1], dating back to Onsager's [2] studies of the isotropic-nematic transition of rigid hard rods using a second-virial approximation. More recent theoretical studies have turned to considering the effects of molecular flexibility on liquid crystal behavior in athermal models of elongated molecules. The effects of flexibility on the isotropic-nematic (I-N) transition of semiflexible "wormlike" chain molecules are fairly well understood, shifting the densities (or concentrations) at the transition to higher values and decreasing the phase gap with increasing degree of flexibility [3–6]. These findings agree qualitatively with experimental results for suspensions of virus particles [7] and also have been applied to thermotropic liquid-crystalline polymers [8,9].

The effects of flexibility on transitions to smectic phases have also been studied. Computer simulations indicate that increasing flexibility also shifts the nematic to smectic-A (N–Sm-A) transition to higher densities [10]. This agrees with predictions of a phenomenological theory described by Tkachenko [11] for very flexible chains, which also indicates that flexibility drives the N–Sm-A transition to be first order while it decreases the smectic period compared to that of rigid rods. These results are supported by experimental findings for virus suspensions [12]. Similar findings have been obtained by van der Schoot [13] in the complementary limit of weak flexibilities, employing an extension of the Khokhlov-Semenov [3,14] theory for wormlike chains. Nonetheless, as discussed in more detail later, we question several aspects of the theory presented in Ref. [13], and believe that further study is warranted. In addition, here we consider the simultaneous shifts of the I-N and N–Sm-A transitions, leading to the finding that sufficient flexibility can suppress the nematic phase and lead to direct isotropic-smectic transitions.

Here we adopt the self-consistent-field theory (SCFT) for wormlike chains [15] with excluded-volume interactions described in the Onsager second-virial approximation, as formulated by Chen *et al.* [5,16]. As noted in Ref. [13], this approximation is probably poor quantitatively in the high volume-fraction regime where smectic phases are expected to occur, but should provide a reasonable qualitative description of smectic structure and phase behavior [17]. We note that related SCFT studies of interfaces and "microphase separation" in fluids of semiflexible wormlike chains have recently been carried out, although mainly employing either Flory-Huggins [18,19] or Maier-Saupe models [20] for the intermolecular interactions. In a recent work [21], we have applied the "SCFT-Onsager" formalism to a model fluid composed of diblock chains (see also [22,23]), where each molecule consists of a flexible (or "coil") part and a rigid (or "rod") part. When the relative fractions of rod and coil segments are comparable, this model was shown to produce smectic-A (i.e., lamellar) phases, analogous to the occurrence of microphase separation in other models of diblock copolymers [18,24,25]. For reasons of both numerical difficulties and (as discussed below) limitations of the model intermolecular interactions, the study in Ref. [21] could not be extended to examine smectic formation in the limit of homogeneous chains each characterized by a single degree of flexibility (or "persistence length" l_p) throughout. Such an examination is the subject of the present work.

*Electronic address: raul@physics.uoguelph.ca

In the original formulation of the Onsager model for nematic phases of wormlike chains [3–5,14], used in subsequent treatments of nonuniform systems [16,21], the excluded-volume interactions between two chain molecules are evaluated by assuming that each polymer chain, of total contour length L, can be viewed as a large number of short, rigid segments that make up the chains. Typically, such a short segment has a length smaller than the persistence length so that it can be considered as a rigid rod, in order to use the Onsager treatment, originally developed for rigid rods. This formalism then reduces to that in Eqs. (4) and (7) in the next section, used in all previous related work [3–5,8,9,16,21]. The Onsager model used in these works typically neglects the effects of the polymer terminal ends, which can be shown to give only corrections of order of magnitude D/L to the isotropic-nematic transition properties, where D is the molecular thickness. However, in highly dense systems where the Onsager excluded-volume interaction leads to a high degree of orientational ordering, the second virial coefficient term for the segment-segment interaction reduces to a magnitude that is comparable to D/L. In view of the fact that the N–Sm-A transition occurs at high density, the inclusion of the end-segment contribution hence becomes important. The influence of terminal or end effects on smectic formation is related to the so-called "shadow" effect described by Tkachenko [11].

This paper is organized as follows. In Sec. II, a complete description of the model and self-consistent-field theory is given, while Sec. III discusses the numerical methods used to solve the theory. In Sec. IV, results are presented for the chain-segment distribution function as well as the phase diagram of the model for systems with different rigidities. We conclude with a summary and discussion in Sec. V.

II. MODEL

We consider a monodisperse fluid of n semiflexible homopolymers, each of contour length L and diameter D, occupying a total volume V. Each homopolymer is characterized by the relative rigidity ξ, equal to the persistence length l_p in units of L. The total average number density n/V is denoted by ρ. In accord with the wormlike chain model for semiflexible chains [5,15,16,18–20,24,26], polymer i is treated as a space curve $\mathbf{r}_i(t)$, with corresponding unit tangent vector $\mathbf{u}_i(t)=L^{-1}d\mathbf{r}_i(t)/dt$, where t varies between 0 and 1.

Jumping immediately to a mean-field treatment, which can be derived by a standard functional-integral method [5,16], the Helmholtz free-energy functional F of our molecular system is given by

$$\beta F = \int D\{\mathbf{r},\mathbf{u}\}\rho_m(\{\mathbf{r},\mathbf{u}\})(\ln[\rho_m(\{\mathbf{r},\mathbf{u}\})] + \beta U(\{\mathbf{r},\mathbf{u}\}) - 1) + \beta F_{int}, \tag{1}$$

where $\beta=1/k_BT$. Here $\rho_m(\{\mathbf{r},\mathbf{u}\})$ is the single-molecule probability distribution function, which satisfies the normalization condition,

$$\int D\{\mathbf{r},\mathbf{u}\}\rho_m(\{\mathbf{r},\mathbf{u}\}) = n. \tag{2}$$

The notation $\{\mathbf{r},\mathbf{u}\}$ stands for the position $\mathbf{r}$ and orientation $\mathbf{u}$ of all segments of a chain molecule; it is useful to picture this as the continuum limit, indexed by the variable t, of a discrete representation in which a molecule has N segments of length $L\mathrm{d}t$ with coordinates $\{\mathbf{r}_1,\mathbf{u}_1,\mathbf{r}_2,\mathbf{u}_2,\ldots,\mathbf{r}_N,\mathbf{u}_N\}$ specifying a $5N$-dimensional phase space, in which $D\{\mathbf{r},\mathbf{u}\}=\{\mathrm{d}\mathbf{r}_1\mathrm{d}\mathbf{u}_1\mathrm{d}\mathbf{r}_2\mathrm{d}\mathbf{u}_2\cdots\mathrm{d}\mathbf{r}_N\mathrm{d}\mathbf{u}_N\}$ can be understood as a volume element in that phase space. The function F_{int} in Eq. (1) is the contribution of intermolecular interactions to the free energy, while $U(\{\mathbf{r},\mathbf{u}\})$ accounts for all "one-body" potentials, including external fields which are not considered in this paper and internal entropic contributions due to the bending fluctuations of the polymers, crucial for describing the effects of flexibility. For the wormlike chain model, this is given by [15]

$$\beta U(\{\mathbf{r},\mathbf{u}\}) = \frac{\xi}{2}\int_0^1 \mathrm{d}t\left|\frac{d\mathbf{u}(t)}{dt}\right|^2. \tag{3}$$

In our previous work [5,16,21], the free energy due to excluded-volume interactions between molecules was taken as

$$\beta F_{int,0} = \frac{\rho^2}{2}\int \mathrm{d}\mathbf{r}\int \mathrm{d}\mathbf{u}\int \mathrm{d}\mathbf{u}'V(\mathbf{u},\mathbf{u}')\phi(\mathbf{r},\mathbf{u})\phi(\mathbf{r},\mathbf{u}'), \tag{4}$$

where the dimensionless contour-averaged segment density $\phi(\mathbf{r},\mathbf{u})$ is defined by

$$\phi(\mathbf{r},\mathbf{u}) = \frac{1}{\rho}\int_0^1 \mathrm{d}t\int D\{\mathbf{r},\mathbf{u}\}\rho_m(\{\mathbf{r},\mathbf{u}\})\delta(\mathbf{r}-\mathbf{r}(t))\delta(\mathbf{u}-\mathbf{u}(t)), \tag{5}$$

which satisfies the normalization condition [following from Eqs. (2) and (5)]

$$\int \mathrm{d}\mathbf{r}\mathrm{d}\mathbf{u}\phi(\mathbf{r},\mathbf{u}) = V. \tag{6}$$

The excluded-volume interaction between two segments, of length $L\mathrm{d}t$ and $L\mathrm{d}t'$ and axial orientations $\mathbf{u}$, $\mathbf{u}'$, $V(\mathbf{u},\mathbf{u}')\mathrm{d}t\mathrm{d}t'$, has previously been taken to be given by the Onsager second-virial approximation, which in the limit of very thin polymers ($L\gg D$) gives rise to [5,14,16,21]

$$V(\mathbf{u},\mathbf{u}') = 2DL^2|\mathbf{u}\times\mathbf{u}'|. \tag{7}$$

Here we propose to extend the above model interaction to account for overlap between the "cylindrical" segments of each molecule (c) with the "terminal (or end) segments" (e) of the other molecules. This adds a contribution to the interaction free energy of

$$\beta\Delta F_{int} = \rho^2 \int d\mathbf{r} \int d\mathbf{u} \int d\mathbf{u}' V_{ce}(\mathbf{u},\mathbf{u}') \times \phi(\mathbf{r},\mathbf{u})[\psi(\mathbf{r},\mathbf{u}',t=0) + \psi(\mathbf{r},\mathbf{u}',t=1)], \quad (8)$$

where, generally, the t-dependent dimensionless segment density is defined by

$$\psi(\mathbf{r},\mathbf{u},t) = \frac{1}{\rho} \int D\{\mathbf{r},\mathbf{u}\}\rho_m(\{\mathbf{r},\mathbf{u}\})\delta(\mathbf{r}-\mathbf{r}(t))\delta(\mathbf{u}-\mathbf{u}(t)). \quad (9)$$

The functions ψ in Eq. (8) are evaluated at $t=0$ and $t=1$ and hence represent the average densities of *terminal* segments. The function $V_{ce}(\mathbf{u},\mathbf{u}')dt$ accounts for the excluded volume between a cylindrical segment of length Ldt with axial orientation $\mathbf{u}$ and an end cap of diameter D, with axial orientation $\mathbf{u}'$ (either a disk or a hemisphere). On dimensional grounds, we see that this should be of order D^2Ldt, hence $V_{ce}(\mathbf{u},\mathbf{u}') \propto D^2L$, in contrast to Eq. (7), for the interaction of cylinders with the terminal segments.

Consider the interaction of a flat end with a cylindrical segment, where the excluded volume can be best represented by that of a disk and a rod. The relative orientation of the two axial vectors prefers to be perpendicular [2], which is different from the segment-segment interaction, where the two axial unit vectors prefer to be parallel. This, however, is not always true for cylinders whose ends are capped with any shape. The excluded volume for spherocylinders, the ends being capped with hemispheres, yields a V_{ce} that is independent of both $\mathbf{u}$ and $\mathbf{u}'$ and given by [8,9],

$$V_{ce}(\mathbf{u},\mathbf{u}') = \frac{\pi L D^2}{2}. \quad (10)$$

While the order of magnitude of this correction is the same as V_{ce} for, say, a flat end, the resulting physical picture is slightly different. Now there is no preferred orientation between a terminal and a cylindrical segment [2]. In either case, driven by the $\mathbf{u}$-dependent end-segment interaction (flat end) or by the $\mathbf{u}$-independent end-segment interaction (hemispherical end), polymer terminals prefer to stay away from the segment-rich region, resulting in smectic-A (Sm-A) formation in which the terminal ends aggregate.

Here we have neglected one other, generally smaller, contribution due to overlap of two terminal segments, which is of order D^3. Henceforth, we take the interaction free energy to be

$$\beta F_{int} = \beta F_{int,0} + \beta\Delta F_{int}. \quad (11)$$

One notes that both interaction contributions $\beta F_{int,0}$ and $\beta\Delta F_{int}$ appear to be spatially "local," i.e., involving products of segment densities evaluated at the *same* position $\mathbf{r}$. This is in apparent contrast to other density-functional theories, e.g., of rigid rods [1,17,27,28], where the interaction free energy at the Onsager second-virial level involves the products of two molecular probability densities at *different* positions $\mathbf{r}$ and $\mathbf{r}'$. The local formulation here is consistent with most theories of polymers [29], however, in which segment-segment interactions are approximated by δ-function contact potentials $\propto\delta(\mathbf{r}'-\mathbf{r})$. Nonetheless, nonlocality is present due to the fact that the segment density $\phi(\mathbf{r},\mathbf{u})$ is *contour-averaged*, see Eq. (5). In the limit of completely rigid molecules, $\xi\to\infty$, it can be shown [30] that the interaction free energy Eq. (11) agrees with the standard formulation for rigid spherocylinders [28] in the second-virial approximation, in the asymptotic limit $L/D\to\infty$, including as a special case the results of Mulder's bifurcation analysis [31] in the limit of perfect alignment, in which all rods are constrained to have the same orientation $\mathbf{u}$. In this constrained limit, the interaction $\beta F_{int,0}$ vanishes and only $\beta\Delta F_{int}$ contributes. Thus, as will be shown later, we recover the rigid-rod results for the N–Sm-A transition in this limit [17,28].

A. Functional minimization

The equilibrium distribution function is obtained by minimizing F with respect to $\rho_m(\{\mathbf{r},\mathbf{u}\})$, subject to the constraint in Eq. (2), which as usual can be taken into account by means of a Lagrange multiplier. Using Eqs. (1), (4), (8), and (11) for F, as well as the relations in Eqs. (5) and (9), we obtain the following equation for $\rho_m(\{\mathbf{r},\mathbf{u}\})$:

$$\rho_m(\{\mathbf{r},\mathbf{u}\}) = \frac{n}{Q} e^{-\beta U(\{\mathbf{r},\mathbf{u}\}) - W(\{\mathbf{r},\mathbf{u}\})}, \quad (12)$$

where

$$Q = \int D\{\mathbf{r},\mathbf{u}\} e^{-\beta U(\{\mathbf{r},\mathbf{u}\}) - W(\{\mathbf{r},\mathbf{u}\})}, \quad (13)$$

and the function $W(\{\mathbf{r},\mathbf{u}\})$ is given by

$$W(\{\mathbf{r},\mathbf{u}\}) = \int_0^1 dt w(\mathbf{r}(t),\mathbf{u}(t)) + w_q(\mathbf{r}(1),\mathbf{u}(1)) + w_q(\mathbf{r}(0),\mathbf{u}(0)), \quad (14)$$

where

$$w(\mathbf{r},\mathbf{u}) = \rho \int d\mathbf{u}' V(\mathbf{u},\mathbf{u}')\phi(\mathbf{r},\mathbf{u}') + \rho \times \int d\mathbf{u}' V_{ce}(\mathbf{u},\mathbf{u}')[\psi(\mathbf{r},\mathbf{u}',0) + \psi(\mathbf{r},\mathbf{u}',1)] \quad (15)$$

and

$$w_q(\mathbf{r},\mathbf{u}) = \rho \int d\mathbf{u}' V_{ce}(\mathbf{u},\mathbf{u}')\phi(\mathbf{r},\mathbf{u}'). \quad (16)$$

Of technical relevance later, for the model of V_{ce} given in Eq. (10), both w_q and the second integral in Eq. (15) for $w(\mathbf{r},\mathbf{u})$ are, in fact, independent of orientation $\mathbf{u}$. This is not the case for a flat cap, which is not considered here, where the same qualitative results are also expected. When we substitute the solution Eq. (12) into the free energy given by Eq. (1), we find that the equilibrium value of βF (denoted βF_{eq}) is given by

$$\beta F_{eq} = (\beta F_{int})_{eq} - \int D\{\mathbf{r},\mathbf{u}\}\rho_m(\{\mathbf{r},\mathbf{u}\})W(\{\mathbf{r},\mathbf{u}\}) - \ln\left(\frac{Q^n}{n!}\right), \tag{17}$$

which, using Eq. (14) and Eqs. (5) and (9), can be written as

$$\beta F_{eq} = (\beta F_{int})_{eq} - \rho \int \mathrm{d}\mathbf{r}\mathrm{d}\mathbf{u}\{w(\mathbf{r},\mathbf{u})\phi(\mathbf{r},\mathbf{u}) + w_q(\mathbf{r},\mathbf{u}) \times [\psi(\mathbf{r},\mathbf{u},0) + \psi(\mathbf{r},\mathbf{u},1)]\} - \ln\left(\frac{Q^n}{n!}\right). \tag{18}$$

Furthermore, substituting Eqs. (15) and (16), this becomes

$$\beta F_{eq} = -(\beta F_{int})_{eq} - \ln\left(\frac{Q^n}{n!}\right), \tag{19}$$

where $(\beta F_{int})_{eq}$ is the equilibrium value of βF_{int} defined by Eqs. (4), (8), and (11), i.e., evaluated using the equilibrium solutions for $\phi(\mathbf{r},\mathbf{u})$ and $\psi(\mathbf{r},\mathbf{u},t)$.

Henceforth, we will absorb the intramolecular bending energy $\beta U(\{\mathbf{r},\mathbf{u}\})$ into the integration element $D\{\mathbf{r},\mathbf{u}\}$ and denote, in agreement with conventional notation [24,26],

$$D\{\mathbf{r},\mathbf{u}\}e^{-\beta U(\{\mathbf{r},\mathbf{u}\})} = D\{\cdot\}. \tag{20}$$

Then, substituting the solution for ρ_m, Eq. (12), into Eq. (5) for $\phi(\mathbf{r},\mathbf{u})$, and using Eqs. (14) and (20), we obtain

$$\phi(\mathbf{r},\mathbf{u}) = \frac{V}{Q}\int_0^1 \mathrm{d}t \int D\{\cdot\} \times e^{-\int_0^1 dt' w(\mathbf{r}(t'),\mathbf{u}(t'))-w_q(\mathbf{r}(1),\mathbf{u}(1))-w_q(\mathbf{r}(0),\mathbf{u}(0))}\delta(\mathbf{r} - \mathbf{r}(t))\delta(\mathbf{u}-\mathbf{u}(t)). \tag{21}$$

This can be expressed in terms of conditional chain-end distribution functions or propagators $q(\mathbf{r},\mathbf{u},t)$ and $q^\dagger(\mathbf{r},\mathbf{u},t)$ as

$$\phi(\mathbf{r},\mathbf{u}) = \frac{V}{Q}\int_0^1 \mathrm{d}t q(\mathbf{r},\mathbf{u},t)q^\dagger(\mathbf{r},\mathbf{u},t), \tag{22}$$

where the propagators are defined as

$$q(\mathbf{r},\mathbf{u},t) = \int D\{\cdot\}_{t'<t}\, e^{-\int_0^t dt' w(\mathbf{r}(t'),\mathbf{u}(t'))-w_q(\mathbf{r}(0),\mathbf{u}(0))}, \tag{23}$$

$$q^\dagger(\mathbf{r},\mathbf{u},t) = \int D\{\cdot\}_{t'>t}\, e^{-\int_t^1 dt' w(\mathbf{r}(t'),\mathbf{u}(t'))-w_q(\mathbf{r}(1),\mathbf{u}(1))}. \tag{24}$$

In both integrals (23) and (24), the coordinates of the chain segment at t are fixed so that $\mathbf{r}(t)=\mathbf{r}$ and $\mathbf{u}(t)=\mathbf{u}$. The notation $D\{\cdot\}_{t'<t}$ means to only integrate $\mathrm{d}\mathbf{r}(t')$ and $\mathrm{d}\mathbf{u}(t')$ for chain segments at $t'<t$. It also follows from the above definition and from Eq. (13) that

$$Q = \int \mathrm{d}\mathbf{r}\mathrm{d}\mathbf{u}q(\mathbf{r},\mathbf{u},t)q^\dagger(\mathbf{r},\mathbf{u},t), \tag{25}$$

where t is arbitrary. Similarly, the general t-dependent segment density is given by

$$\psi(\mathbf{r},\mathbf{u},t) = \frac{V}{Q}q(\mathbf{r},\mathbf{u},t)q^\dagger(\mathbf{r},\mathbf{u},t). \tag{26}$$

The definitions of the propagators $q(\mathbf{r},\mathbf{u},t)$ and $q^\dagger(\mathbf{r},\mathbf{u},t)$ in Eqs. (23) and (24), respectively, are consistent with those of earlier theories [18,19,21], except for the additional terms in the arguments of the exponentials involving the functions $w_q(\mathbf{r}(0),\mathbf{u}(0))$ and $w_q(\mathbf{r}(1),\mathbf{u}(1))$. From those equations, it follows that

$$q(\mathbf{r},\mathbf{u},t\to 0) = q^\dagger(\mathbf{r},\mathbf{u},t\to 1) = e^{-w_q(\mathbf{r},\mathbf{u})}, \tag{27}$$

while otherwise the diffusionlike equations for $q(\mathbf{r},\mathbf{u},t)$ and $q^\dagger(\mathbf{r},\mathbf{u},t)$ used in earlier theories of wormlike chains are unchanged, namely

$$\frac{\partial}{\partial t}q(\mathbf{r},\mathbf{u},t) = \left[-L\mathbf{u}\cdot\boldsymbol{\nabla}_\mathbf{r} + \frac{1}{2\xi}\boldsymbol{\nabla}_\mathbf{u}^2 - w(\mathbf{r},\mathbf{u})\right]q(\mathbf{r},\mathbf{u},t), \tag{28}$$

$$\frac{\partial}{\partial t}q^\dagger(\mathbf{r},\mathbf{u},t) = \left[-L\mathbf{u}\cdot\boldsymbol{\nabla}_\mathbf{r} - \frac{1}{2\xi}\boldsymbol{\nabla}_\mathbf{u}^2 + w(\mathbf{r},\mathbf{u})\right]q^\dagger(\mathbf{r},\mathbf{u},t). \tag{29}$$

For the present case of homopolymers, we note that, in fact, $q^\dagger(\mathbf{r},\mathbf{u},t)=q(\mathbf{r},-\mathbf{u},1-t)$.

We comment here on the closely related approach of van der Schoot [13]. This is also based on the Onsager second-virial approximation, although it takes the total interaction free energy βF_{int} to be given by the *nonlocal* generalization of Eq. (4) [see discussion following Eq. (11)], involving products of the *contour-averaged* segment densities $\rho^2\phi(\mathbf{r},\mathbf{u})\phi(\mathbf{r}',\mathbf{u}')$ and with $-V(\mathbf{u},\mathbf{u}')$ replaced by the full Mayer function for rigid spherocylinders. However, there is no explicit analysis of contour-averaging, i.e., no account is taken of the t dependence of the propagators as in Eqs. (28) and (29). This is due to the fact that van der Schoot applies a perturbation expansion to first order in $1/\xi$, following an approach used by Khokhlov and Semenov [3] for uniform systems, which treats both the Laplacian term $\boldsymbol{\nabla}_\mathbf{u}^2/2\xi$ and the spatial-gradient term $L\mathbf{u}\cdot\boldsymbol{\nabla}_\mathbf{r}$ in Eqs. (28) and (29) as small perturbations. The spatial-gradient term can, obviously, be neglected for a uniform system, but it can be shown [30] that it is crucial for obtaining correct results for rigid rods in the limit $\xi\gg 1$, the limit which is, after all, the basis for the perturbation treatment. In the present formulation, this is the only term coupling positional and orientational degrees of freedom.

III. SELF-CONSISTENT CALCULATIONS

To proceed with the solution of the mean-field equations, we now specialize to situations in which the densities vary in only one spatial dimension, which is chosen to be the z direction. Here, as in previous work [16,21], we represent the orientational ($\mathbf{u}$) dependencies of the functions ϕ, w, q, and $q^\dagger$ using expansions in spherical harmonics $Y_{l,m}(\mathbf{u})$. Furthermore, we shall only consider liquid-crystalline phases such as nematic and smectic-A with uniaxial (i.e., azimuthal) sym-

metry about the z axis, and hence we need only harmonics with $m=0$ (proportional to Legendre polynomials),

$$\phi(z,\mathbf{u}) = \sum_l \phi_l(z) Y_{l,0}(\mathbf{u}),$$

$$w(z,\mathbf{u}) = \sum_l w_l(z) Y_{l,0}(\mathbf{u}),$$

$$q(z,\mathbf{u},t) = \sum_l q_l(z,t) Y_{l,0}(\mathbf{u}),$$

$$q^\dagger(z,\mathbf{u},t) = \sum_l q_l^\dagger(z,t) Y_{l,0}(\mathbf{u}). \tag{30}$$

Next, we expand the kernel $|\mathbf{u}\times\mathbf{u}'|$ using the addition theorem for spherical harmonics [16,32],

$$|\mathbf{u}\times\mathbf{u}'| = \sum_{l,m} \frac{4\pi}{2l+1} d_l Y_{l,m}(\mathbf{u}) Y^*_{l,m}(\mathbf{u}') \tag{31}$$

with

$$d_l = 0, \quad l \text{ odd},$$

$$d_0 = \frac{\pi}{4},$$

$$d_{2k} = -\frac{\pi(4k+1)(2k)!(2k-2)!}{2^{4k+1}(k-1)!k!k!(k+1)!}, \quad k = 1,2,3,\ldots . \tag{32}$$

Inserting these formulas into the free energy (19), the latter can be expressed as

$$\beta F = -\rho A \sum_l \left[\frac{4\pi C d_l}{2l+1}\right] \int \mathrm{d}z \phi_l(\mathbf{r})^2 - \rho A \frac{\sqrt{4\pi} C_2 V}{Q} \int \mathrm{d}z \phi_0(z) \times [q_0(z,1) q_0^\dagger(z,1) + q_0(z,0) q_0^\dagger(z,0)] - \ln \frac{Q^n}{n!}, \tag{33}$$

where $C \equiv \rho D L^2$ and $C_2 = \rho V_{ce} \equiv \pi \rho L D^2/2$. The mean-field equations (15) and (22) are

$$w_l(z) = \frac{8\pi d_l C}{2l+1}\phi_l(z) + \frac{\sqrt{4\pi} C_2 V}{Q}[q_0(z,1) q_0^\dagger(z,1) + q_0(z,0) q_0^\dagger(z,0)]\delta_{l,0}, \tag{34}$$

$$\phi_l(z) = \frac{V}{Q} \sum_{l',l''} \int_0^1 \mathrm{d}t q_{l'}^\dagger(z,t) q_{l''}(z,t) \times \sqrt{\frac{(2l''+1)(2l'+1)}{4\pi(2l+1)}} (C^{l'',l',l}_{0,0,0})^2 \tag{35}$$

with

$$Q = A \sum_l \int \mathrm{d}z q_l^\dagger(z,t) q_l(z,t). \tag{36}$$

Here A is the cross-sectional area of the system in the x and y directions. The $C^{l'',l',l}_{0,0,0}$ are Clebsch-Gordan coefficients, and we have used a result for the integral of three spherical harmonics [33]. In terms of the projections $q_l(z,t)$, the diffusionlike equation (28) becomes

$$\frac{\partial}{\partial t} q_l(z,t) = -L \sum_{l'} \sqrt{\frac{2l'+1}{2l+1}} (C^{1,l',l}_{0,0,0})^2 \frac{\partial}{\partial z} q_{l'}(z,t) - \frac{1}{2\xi} l(l+1) q_l(z,t) - \sum_{l',l''} \sqrt{\frac{(2l''+1)(2l'+1)}{4\pi(2l+1)}} \times (C^{l'',l',l}_{0,0,0})^2 \times w_{l'}(z) q_{l''}(z,t) \tag{37}$$

with initial conditions, following from Eq. (27),

$$q_0(z,0) = \sqrt{4\pi} e^{-w_q(z)} = \sqrt{4\pi} e^{-\sqrt{4\pi} C_2 \phi_0(z)},$$

$$q_l(z,0) = 0, \quad l > 0, \tag{38}$$

where we have used the fact that w_q is independent of $\mathbf{u}$ as well as Eq. (16). Analogous equations apply to $q^\dagger(z,\mathbf{u},t)$.

The computational methods used in solving the theory are similar to those of Ref. [21], based on use of a forward time centered space (FTCS) scheme [34] for obtaining solutions of the diffusionlike equation (37). The fields and densities are determined self-consistently according to Eqs. (34), (35), and (37) using a fixed-point iteration algorithm with variable mixing parameters for successive iterations. In the present work, calculations were performed on a one-dimensional grid with periodic boundary conditions, a spatial discretization of $\mathrm{d}z/d = 0.02$, where d is the smectic period, and a contour discretization of $\mathrm{d}t = 1/1500$. All spherical-harmonic expansions were truncated after $l = 12$.

The use of the spherical-harmonic series representations in Eq. (30) results in one limitation on our calculations, namely for describing states with very sharply peaked orientational distributions about the director axis (i.e., the z axis). In practice, we find this restricts our calculations to small aspect ratios $L/D < 10$, although within this range we do find significant trends as described in the next section.

IV. RESULTS

The first results of the present calculations are the distribution functions $\psi(z,u_z,t)$ for the density of segments at point t along a chain, in terms of the segment position z and orientation $u_z \equiv \cos(\theta)$, where θ is the angle between the segment axis and the z axis, indicating the type of structure which is present. The distribution functions for segments at several different t values are presented in Fig. 1, for parameter values of $C=9$, $C_2=1.8$, and rigidity $\xi=5$. These values lie in the smectic region of the model, with a corresponding optimal period of $d=1.2L$. The graphs show, firstly, that all segments for this value of ξ are sharply peaked at orientations $u_z=\pm 1$. The graphs of the distribution function have been made by setting the origin in z at the midplane of the smectic layers, i.e., where $\psi(z,u_z,t=0.5)$ is maximum. They are also consistent with two general symmetry relations which can be derived from Eqs. (26), (28), and (29), namely $\psi(z,u_z,t) = \psi(z,-u_z,1-t)$ and $\psi(z,u_z,t) = \psi(d-z,u_z,1-t)$.

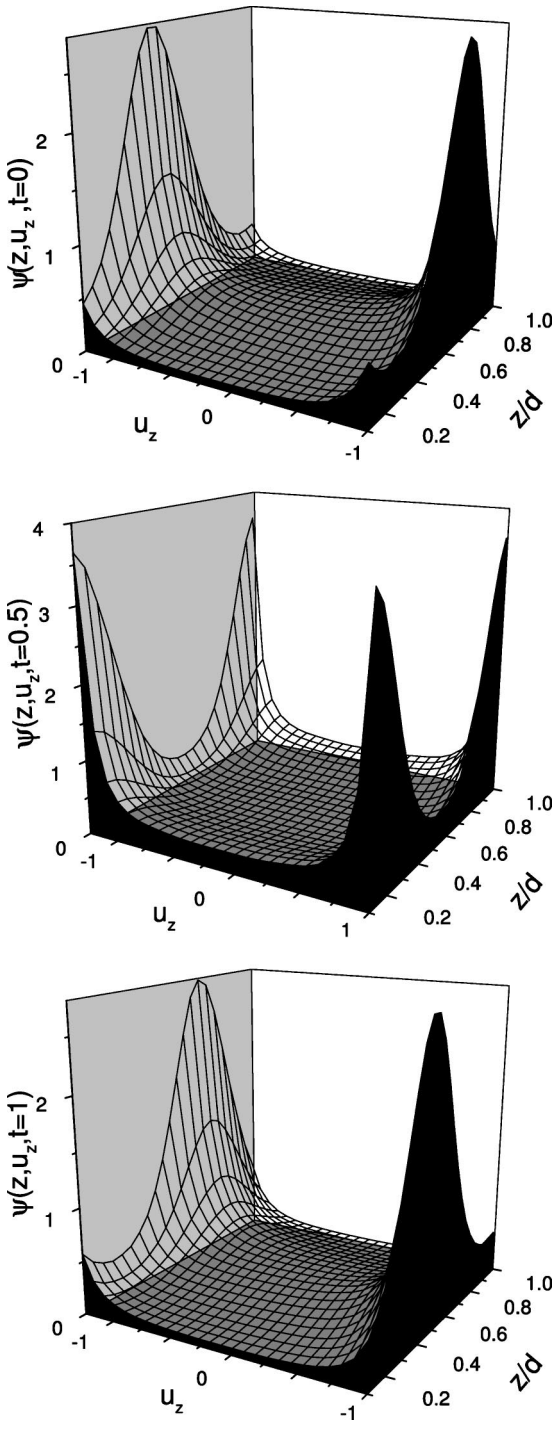

FIG. 1. The distribution function $\psi(z,u_z,t)$ for segments at different values of t, corresponding to parameter values $C=9$, $C_2=1.8$, $\xi=5$, where the equilibrium period is $d=1.2L$.

Notice that the maxima (versus z) of $\psi(z,u_z,t=0.5)$ coincide approximately with the minima of $\psi(z,u_z,t=0)$ and $\psi(z,u_z,t=1)$. Comparing the results for $t=0$ and $t=1$ at the most probable orientation (either $u_z=1$ or $u_z=-1$), the closest distance between adjacent maxima of $\psi(z,u_z,t)$ is approximately $0.33L$, representing the width of the depletion zone between successive smectic layers. The corresponding maximum distance between adjacent maxima of $\psi(z,u_z,t)$ is $d-0.33L=0.87L$, which can be interpreted as the thickness of the high-density smectic layer.

TABLE I. Isotropic-nematic coexistence densities (C_{nem},C_{iso}) for several values of the relative rigidity ξ.

	Results from Ref. [5]		Present work	
Chain rigidity ξ	C_{iso}	C_{nem}	C_{iso}	C_{nem}
∞	4.19	5.33	4.18	5.36
10	4.74	5.54	4.78	5.49
5	5.26	5.96	5.21	5.90
3	5.89	6.53	5.89	6.52
1	9.69	10.39	9.61	11.21

We next turn to the phase boundaries of the model. To determine the coexistence regions of first-order phase transitions, we performed double-tangent constructions on curves of the free energy per volume $\beta F/V$ [21]. Omitting terms linear in C (which yield constants when the derivative $\partial/\partial C$ is taken), we obtain from Eqs. (33) and (38)

$$\frac{\beta F}{V}\propto\frac{\beta FC}{n}=-4\pi C^2\left(\frac{A}{V}\right)\sum_l\frac{d_l}{2l+1}\int dz\,\phi_l^2(z)$$
$$-\frac{4\pi C_2CA}{Q}\int dz\,\phi_0(z)e^{-\sqrt{4\pi}C_2\phi_0(z)}[q_0(z,1)+q_0^+(z,0)]$$
$$-C\ln\frac{Q}{V}+C\ln C, \tag{39}$$

where we have used Stirling's approximation for the factorial. Results for the coexisting values of C at the isotropic-nematic transition for different rigidities ξ are summarized in Table I and are in excellent agreement with previous results [5]. Although the free energy of the uniform isotropic and nematic phases depends on the parameter C_2, with a term varying in proportion to ρC_2, we find that the C_2 dependence has a negligible effect (within our numerical uncertainties) on the coexisting values of C.

The phase diagram of the model was studied in terms of the aspect ratio L/D and the packing fraction η, which is defined as [28]

$$\eta=\frac{\pi\rho LD^2}{4}\left(1+\frac{2}{3}\frac{D}{L}\right). \tag{40}$$

These variables are related to the parameters C and C_2 through the relations

$$\frac{L}{D}=\frac{\pi}{2}\frac{C}{C_2},\quad \eta=\frac{C_2}{2}\left(1+\frac{4}{3\pi}\frac{C_2}{C}\right). \tag{41}$$

Additionally, there are regions where the nematic-smectic (N–Sm-A) transition is found to be second order. The location of this transition line has been determined by the behavior of the smectic order parameter defined as

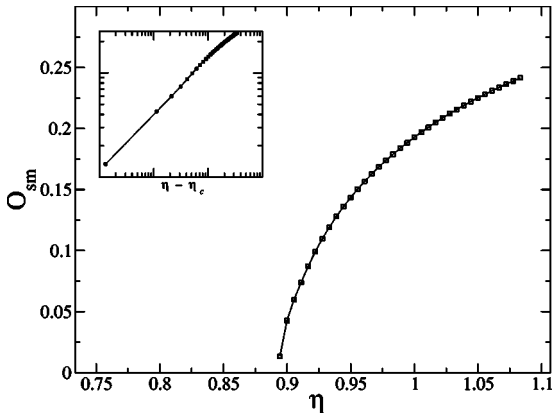

FIG. 2. Order-parameter behavior close to the nematic-smectic critical point of rigid rods ($\xi=\infty$) with $L/D=7.5$. Inset: log-log diagram of the order-parameter variation with distance to the critical point [O_{sm} vs $(\eta-\eta_c)$].

$$O_{sm}=\left[\frac{1}{d}\int_0^d \mathrm{dz}[\sqrt{4\pi}\phi_0(z)-1]^2\right]^{1/2}. \tag{42}$$

Trivially, O_{sm} vanishes in the isotropic and nematic phases and should differ from zero in the smectic phase. To accurately obtain the transition points, we studied the vanishing of O_{sm} as the packing fraction η approaches its critical value η_c, while keeping L/D constant. The behavior of the order parameter O_{sm} as a function of η for a typical second-order N–Sm-A transition is shown in Fig. 2. According to mean-field theory, the order parameter should vanish following a power-law decay,

$$O_{sm}\sim(\eta-\eta_c)^{1/2}. \tag{43}$$

The smooth parabolic shape of the curves in Fig. 2 and the logarithmic fit, included as an inset, are consistent with this power-law behavior. In these cases, the N–Sm-A transition points η_c were determined by fitting the data values O_{sm} versus η with the above formula. In all cases, the data used corresponded with the equilibrium period, i.e., the value of d which minimizes the free energy per volume.

The particular case of infinitely rigid molecules ($\xi=\infty$, i.e., rods) was first studied. Results for the phase boundaries of η versus L/D are given in Fig. 3(a). The solid and dashed lines show the phase coexistence region for first-order transitions and the critical packing fraction η_c for second-order transitions, respectively. The optimal smectic periods were always in the interval $1.20<d/L<1.26$. As a comparison, the asymptotic ($L/D\to\infty$) results of Poniewierski's bifurcation analysis [28] of the N–Sm-A transition in the Onsager approximation are also shown, which are seen to be in close agreement with the present results for all L/D values. We note that Poniewierski's analysis includes orientational fluctuations which are suppressed in, and produce slight differences from, the analysis of Mulder [31] in the perfectly aligned limit. For $L/D>5$, the N–Sm-A transition is found to be second order, while for smaller values of L/D a narrow nematic-smectic coexistence region emerges, so that $L/D=5$ is a tricritical point. For $L/D<4.2$, the N–Sm-A transition is preempted and a direct isotropic-smectic (I–Sm-A) transition occurs. These results can be compared with the Monte Carlo simulation results of Bolhuis and Frenkel [35], who found the N–Sm-A-I triple point to be at $L/D=3.7$ while being inconclusive about the precise location of the

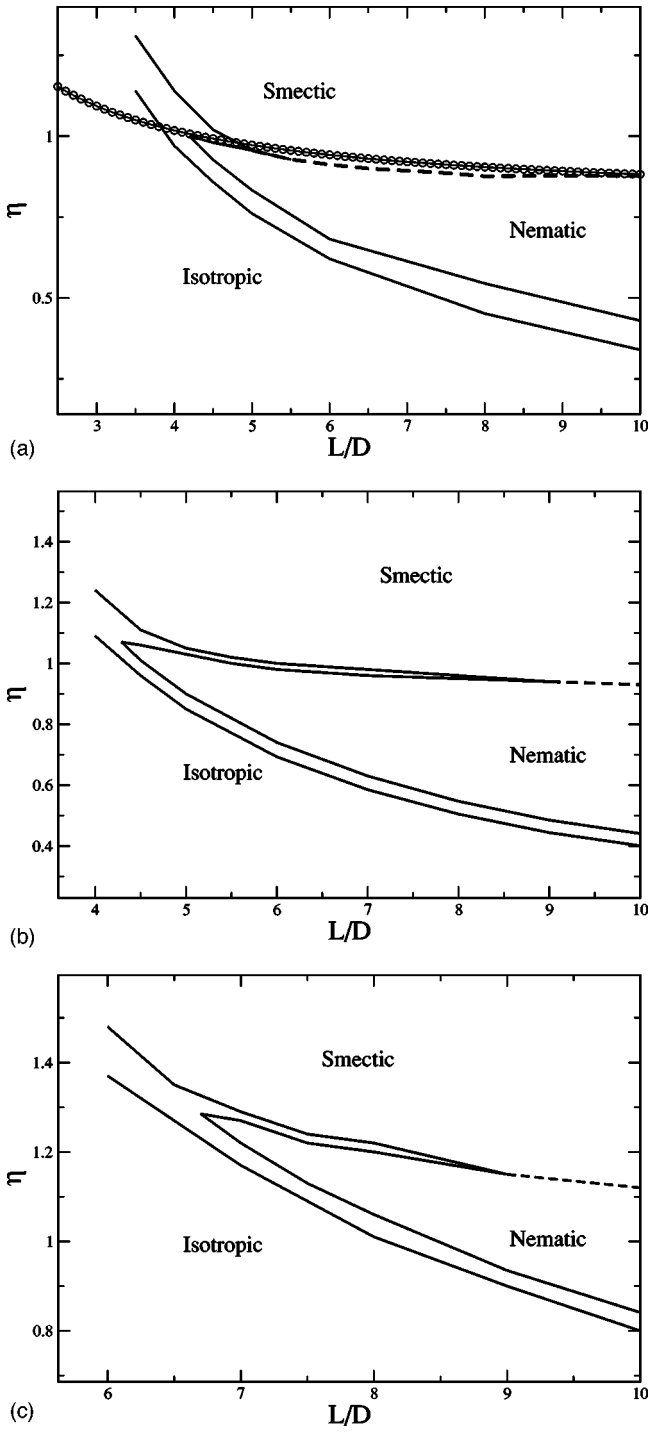

FIG. 3. Phase diagrams for systems with different rigidities: (a) infinitely rigid molecules, $\xi=\infty$, (b) $\xi=10$, and (c) $\xi=1$. The solid and dashed lines define the coexistence regions of first-order phase transitions and the critical packing fraction η_c for second-order phase transitions, respectively. In (a), the points gives the results of Poniewierski's [28] asymptotic analysis.

TABLE II. Triple-point values of L/D and η for several values of the relative rigidity ξ.

Chain rigidity ξ	∞	10	5	3	1
Triple point $(L/D;\eta)$	(4.2;1.00)	(4.3;1.06)	(4.7;1.10)	(5.5;1.18)	(6.7;1.28)

N–Sm-A tricritical point. More recent studies by Polson and Frenkel [36] indicate that the N–Sm-A transition of rigid rods is first order for all aspect ratios. These discrepancies of the present results are presumably due to its basis in the Onsager approximation, as discussed further in Sec. V.

In Figs. 3(b) and 3(c), the phase diagrams are shown for two finite rigidities ξ. As the flexibility $1/\xi$ of the polymer increases, the N–Sm-A transition moves to higher values of both η and L/D. Moreover, the optimal period d of the smectic phase generally decreases as the flexibility increases. For the semiflexible chains ($\xi \neq \infty$), the optimal period was always in the interval $1.04 < d/L < 1.22$. The coexistence values η_N and η_A are seen to decrease as L/D increases, but as mentioned earlier, we are unable to extend our calculations beyond $L/D=10$. For $L/D>9$, the N–Sm-A transition is found to be second order (within our numerical uncertainties). For smaller aspect ratios, this transition is weakly first order until a N–Sm-A-I triple point is encountered. As in the rigid case, below the triple point a direct I–Sm-A transition occurs. The coordinates $(L/D, \eta)$ of the triple point for systems with different rigidities are contained in Table II.

The N–Sm-A transition line in terms of η versus $1/\xi$ is plotted in Fig. 4 for the value $L/D=6$ (solid line). In this figure, the dashed line represents the simulation results obtained by Bladon and Frenkel [10] for a model of jointed spherocylinders with the same L/D value (fitted to the equation proposed by van der Schoot [13], so it is actually drawn over a wider range of $1/\xi$ values than examined in Ref. [10]). The dotted curve shows the results of the asymptotic

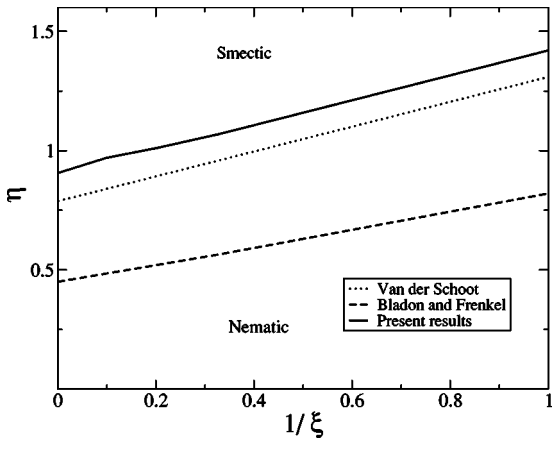

FIG. 4. The nematic-smectic transition (η vs $1/\xi$) for the case of $L/D=6$ (solid line). In the case of first-order transitions, the line represents the values $(\eta_N+\eta_A)/2$. The dashed curve represents the simulation results obtained by Bladon and Frenkel [10], while the dotted curve describes the asymptotic results of Ref. [13].

$(L/D \to \infty)$ second-virial approximation described by van der Schoot [13], which partially agrees with our results. The fact that the N–Sm-A transition predicted by second-virial approximations occurs at higher packing fraction than obtained from simulations [10] is not unexpected (see the next section).

V. SUMMARY AND CONCLUSIONS

The present work generalizes previous studies of liquid-crystalline ordering of homogeneous semiflexible polymers resulting from excluded-volume effects, originated by Khokhlov and Semenov [3,14], to account for the formation of smectic-A phases. This is done by adding an effective interaction term, in a second-virial approximation, which describes the excluded volume between wormlike cylindrical segments and terminal (or end) segments of the polymer molecules. This work provides a more microscopic perspective of the "shadow effect" formulated by Tkachenko [11]. In addition, compared with the coarse-grained description in Ref. [11], the present work explicitly includes the contributions due to orientational degrees of freedom and thus accounts for the occurrence of direct isotropic to smectic-A transitions. For infinitely rigid molecules, our results for the N–Sm-A transition are consistent with those derived by Poniewierski [28] by bifurcation analysis in the large L/D limit, although for numerical reasons the present study is limited to rather small aspect ratios $L/D<10$.

Our main findings are that flexibility ($\xi<\infty$) shifts the N–Sm-A transition and the N–Sm-A-I triple point to higher values of the density η and aspect ratio L/D, decreases the smectic period, and increases the range over which the N–Sm-A transition is first order, all of which are in accord with the predictions of Refs. [11,13] as well as the computer simulation studies of Ref. [10]. In addition, we show via the shift of the N–Sm-A-I triple point to higher density and L/D with decreasing ξ that the nematic phase is gradually eliminated by increasing flexibility.

There are two aspects of the theory discussed here which need to be refined. The first is the treatment of orientational contributions; the spherical-harmonic expansions in Eq. (30) do not converge well for strongly ordered states, which in practice emerge, for the rigidities considered here, at aspect ratios $L/D>10$. (We note that *effective* aspect ratios such as for the virus suspensions studied in Ref. [12] range from 30 to 70.) To overcome this will likely require the use of a real-space discretization of the orientations as in Ref. [5]. We also must consider extensions beyond the second-virial approximation, which in principle is limited to volume fractions $\eta \ll 1$, in order to improve the accuracy of the theory. The latter results in several artifacts, such as predictions of the volume fraction η at the various phase boundaries in

Figs. 3 and 4 which exceed the physical close-packed limit $\eta_{cp} \approx 0.91$, and possibly the presence of the N–Sm-A tricritical points [28]. In reality, the volume fractions at the N–Sm-A transition should "saturate" at values of η below η_{cp} [11,12]. In principle, methods such as that due to Parsons and Lee [37–39] or based on "fundamental measure theory" [40] can be applied to this question, although the use of these methods for nonuniform, orientationally ordered systems still needs significant development.

ACKNOWLEDGMENT

This work was supported by the Natural Sciences and Engineering Research Council (Canada) (NSERC).

[1] M. P. Allen, G. T. Evans, D. Frenkel, and B. M. Mulder, Adv. Chem. Phys. **86**, 1 (1993).
[2] L. Onsager, Ann. N.Y. Acad. Sci. **51**, 627 (1949).
[3] A. R. Khokhlov and A. N. Semenov, Physica A **112**, 605 (1982).
[4] T. Odijk, Macromolecules **19**, 2313 (1986).
[5] Z. Y. Chen, Macromolecules **26**, 3419 (1993).
[6] M. Dijkstra and D. Frenkel, Phys. Rev. E **51**, 5891 (1995).
[7] J. Tang and S. Fraden, Liq. Cryst. **19**, 459 (1995).
[8] T. Sato and A. Teramoto, Adv. Polym. Sci. **126**, 85 (1996).
[9] D. B. DuPre and S.-J. Yang, J. Chem. Phys. **94**, 7466 (1991).
[10] P. Bladon and D. Frenkel, J. Phys.: Condens. Matter **8**, 9445 (1996).
[11] A. V. Tkachenko, Phys. Rev. Lett. **77**, 4218 (1996).
[12] Z. Dogic and S. Fraden, Phys. Rev. Lett. **78**, 2417 (1997).
[13] P. van der Schoot, J. Phys. II **6**, 1557 (1996).
[14] A. N. Semenov and A. R. Khokhlov, Sov. Phys. Usp. **31**, 988 (1988).
[15] N. Saito, K. Takahashi, and Y. Yunoki, J. Phys. Soc. Jpn. **22**, 219 (1967).
[16] S.-M. Cui, O. Akcakir, and Z. Y. Chen, Phys. Rev. E **51**, 4548 (1995).
[17] R. van Roij, P. Bolhuis, B. Mulder, and D. Frenkel, Phys. Rev. E **52**, R1277 (1995).
[18] M. W. Matsen, J. Chem. Phys. **104**, 7758 (1996).
[19] D. C. Morse and G. H. Fredrickson, Phys. Rev. Lett. **73**, 3235 (1994).
[20] R. R. Netz and M. Schick, Phys. Rev. Lett. **77**, 302 (1996); M. Müller and M. Schick, Macromolecules **29**, 8900 (1996).
[21] D. Düchs and D. E. Sullivan, J. Phys.: Condens. Matter **14**, 12 189 (2002).
[22] A. N. Semenov and S. V. Vasilenko, Sov. Phys. JETP **63**, 70 (1986).
[23] M. W. Matsen and C. Barrett, J. Chem. Phys. **109**, 4108 (1998).
[24] M. W. Matsen, J. Phys.: Condens. Matter **14**, R21 (2002).
[25] P. P. F. Wessels and B. M. Mulder, Phys. Rev. E **70**, 031503 (2004).
[26] F. Schmid, J. Phys.: Condens. Matter **10**, 1805 (1998).
[27] A. M. Somoza and P. Tarazona, Phys. Rev. A **41**, 965 (1990).
[28] A. Poniewierski, Phys. Rev. A **45**, 5605 (1992).
[29] H. Yamakawa, *Modern Theory of Polymer Solutions* (Harper and Row, New York, 1971).
[30] R. Cruz Hidalgo, D. E. Sullivan, and J. Z. Y. Chen (unpublished).
[31] B. Mulder, Phys. Rev. A **35**, 3095 (1987).
[32] G. J. Vroege and T. Odijk, Macromolecules **21**, 2848 (1988).
[33] C. G. Gray and K. E. Gubbins, *Theory of Molecular Fluids: Vol. 1: Fundamentals* (Clarendon Press, Oxford, 1984).
[34] W. H. Press, B. P. Flannery, S. A. Teukolsky, and W. T. Vetterling, *Numerical Recipes* (Cambridge University Press, Cambridge, 1986).
[35] P. Bolhuis and D. Frenkel, J. Chem. Phys. **106**, 666 (1997).
[36] J. M. Polson and D. Frenkel, Phys. Rev. E **56**, R6260 (1997).
[37] J. D. Parsons, Phys. Rev. A **19**, 1225 (1979).
[38] S.-D. Lee, J. Chem. Phys. **87**, 4972 (1987).
[39] E. Velasco, L. Mederos, and D. E. Sullivan, Phys. Rev. E **62**, 3708 (2000); **66**, 021708 (2002).
[40] G. Cinacchi and F. Schmid, J. Phys.: Condens. Matter **14**, 12 223 (2002).